



# Allowance for thermodynamic nonideality in the characterization of protein interactions by spectral techniques

Peter R. Wills<sup>a</sup>, Donald J. Winzor<sup>b,\*</sup>

<sup>a</sup> 37 Fairlands Avenue, Waterview, Auckland 1026, New Zealand

<sup>b</sup> School of Chemistry and Molecular Biosciences, University of Queensland, Brisbane, Queensland 4072, Australia

## ARTICLE INFO

### Article history:

Received 1 March 2011

Received in revised form 12 April 2011

Accepted 12 April 2011

Available online 19 April 2011

### Keywords:

Difference spectroscopy

Fluorescence quenching

Molecular crowding

Protein–protein interactions

Thermodynamic nonideality

## ABSTRACT

Theory is developed for the characterization of protein interactions by spectral techniques, where the constraints of constant temperature and pressure demand that thermodynamic activity be defined on the molal concentration scale. The customary practice of defining the equilibrium constant ( $K$ ) on a molar basis is accommodated by developing expressions to convert those experimental values ( $K_{\text{molar}}$ ) to their thermodynamically more rigorous counterparts ( $K_{\text{molal}}$ ). Such procedures are illustrated by reanalysis of published results for the effects of molecular crowding agents on the isomerisation of  $\alpha$ -chymotrypsin and reversible complex formation between catalase and superoxide dismutase. Although those reanalyses have led to only minor refinements of the quantitative interpretation, it is clearly preferable to adopt thermodynamic rigor throughout future spectral studies by employing the molal concentration scale from the outset.

© 2011 Elsevier B.V. All rights reserved.

## 1. Introduction

Techniques such as difference spectroscopy and fluorescence quenching are extremely useful for the quantitative characterization of strong interactions because of their capacity to accommodate the low concentration ranges under which the equilibrium coexistence of complex(es) and reactants occurs. Because these interactions are therefore being studied under conditions approaching thermodynamic ideality, there is no restriction on the concentration scale that can be used for the determination of an equilibrium constant. Strictly speaking, chemical potentials vary with the logarithm of molal rather than molar concentrations under normal laboratory constraints of constant temperature and pressure, even in the ideal limit [1–3]; but this is of little practical significance and the molar concentration scale is invariably used regardless. However, problems arise in attempts to characterize the same interaction in the presence of high concentrations of molecular crowding agents (inert solutes), which give rise not only to thermodynamic nonideality of the system (the reason for their inclusion) but also to a significant difference between concentrations defined on the molal and molar scales. In the absence of crowding agents the magnitude of the molar equilibrium constant defined by spectral studies can certainly be taken as its molal counterpart because the molar and molal concentrations are identical except for the vanishingly small difference between the volumes of equal masses

of solution and solvent. On the other hand, the interaction in the crowded environments should be characterized in terms of a molal association constant before any statistical–mechanical interpretation of the ratio of equilibrium constants is attempted.

This investigation develops the theoretical expressions required for statistical–mechanical interpretation of thermodynamic nonideality in spectral studies of protein isomerization and protein–protein interactions, and also illustrates their application to (i) the crowding effect of sucrose on the isomerization of  $\alpha$ -chymotrypsin [4,5], and (ii) the corresponding effects of dextran and polyethylene glycol on the interaction between catalase and superoxide dismutase [6].

## 2. Theoretical considerations

The chemical potential of a solute in an ideal solution can be expressed in terms of the logarithm of its concentration, but even minor deviations from ideality require the replacement of the concentration with a *thermodynamic activity*, and then the familiar equation must be written in the form

$$(\mu_i)_{T,P} = (\mu_i^0)_{T,P} + RT \ln a_i \quad (1)$$

Even in the case of an ideal solution, it is not enough to specify just the concentration of the solute in order to calculate its chemical potential. The values of some other thermodynamic parameters, such as temperature  $T$  and pressure  $P$ , must also be taken into account. However, it turns out that for a perfectly ideal solution under normal

\* Corresponding author. Fax: +61 7 3365 4699.

E-mail address: [d.winzor@uq.edu.au](mailto:d.winzor@uq.edu.au) (D.J. Winzor).

laboratory conditions of constant temperature and pressure, the activity  $a_i$  defined in Eq. (1) corresponds exactly to the molal concentration  $m_i$  [1,2]. Under these circumstances  $a_i$  is most appropriately and conveniently written as the product of molality and a dimensionless activity coefficient  $\gamma_i$  which approaches unity in the limit  $m_i \rightarrow 0$  [Eq. (2)].

$$a_i = \gamma_i m_i \quad (2)$$

On the other hand, if the temperature  $T$  and chemical potential  $\mu_s$  of solvent  $S$  are kept constant while the solute concentration is varied, as in an osmotic pressure experiment, then one must define a thermodynamic activity  $z_i$  in terms of these different constraints and  $z_i$  reduces to the *molar* concentration  $C_i$  in the case of a perfectly ideal solution. The convenience of  $z_i$  arises from its relationship to the osmotic pressure, which, for a non-ideal solution, can be written straightforwardly as a virial expansion in molar concentrations.

Under the constraints of constant  $T$  and  $P$ , the counterpart of the osmotic virial expansion is, for a thermodynamically non-ideal system comprising a solvent  $S$  and two solutes ( $i, j$ ),

$$-\left[(\mu_s)_{T,P} - (\mu_s^0)_{T,P}\right] / (RT) = m_i + m_j + C_{ii}m_i + C_{ij}m_i m_j + C_{jj}m_j + \dots \quad (3)$$

where  $\mu_s^0$  is the chemical potential of pure solvent. [Note that the double subscripts on the coefficients in Eq. (3) obviate confusion with molar concentrations that have only a single subscript.] The activity coefficient  $\gamma_i$  for each of the solute species, as it is defined in Eq. (2), can be related to the coefficients appearing in Eq. (3), ( $C_{ii}$ ,  $C_{ij}$ , etc.) through the equation [1,2]

$$\gamma_i = \exp(2C_{ii}m_i + C_{ij}m_j + \dots) \quad (4)$$

Although there is generally no simple specification of  $C_{ii}$ ,  $C_{ij}$ , etc., in terms of elementary molecular quantities, they are, for aqueous solutions, related to the classical second osmotic virial coefficients ( $B_{ii}$ ,  $B_{ij}$ , etc.) because of the essential incompressibility of such systems. Specifically,

$$C_{ii} = (B_{ii} - M_i \bar{v}_i) \rho_s \quad (5a)$$

$$C_{ij} = (B_{ij} - M_i \bar{v}_i - M_j \bar{v}_j) \rho_s \quad (5b)$$

in which  $M_i$  and  $\bar{v}_i$  are the molar mass and partial specific volume of species  $i$ , and  $\rho_s$  the solvent density.

For incompressible ternary solutions the use of the relationship

$$m_i \rho_s = C_i / (1 - M_i \bar{v}_i C_i - M_j \bar{v}_j C_j) \quad (6)$$

certainly allows expression of the molality  $m_i$  in terms of molar concentration  $C_i$ ; but the product  $m_i \rho_s$  (measured in units of moles of solute per litre of pure solvent) remains a molal parameter even though its physical dimensions (amount of solute per unit volume) are the same as those of molarity (measured in units of moles of solute per litre of solution). However, for near ideal systems the combined contributions of the reactant and product species to the solution volume is less than 0.1%; and hence we shall disregard the difference between solvent and solution volumes in the absence of any cosolute included as a crowding agent to impart nonideality to the systems. Because the molar concentration scale is used routinely in spectral studies of nonideality effects on protein interactions, we now derive expressions to assess the consequences of such action on the interpretation of results for two types of equilibria, namely protein isomerization and protein–protein interaction.

## 2.1. Expressions for nonideal protein isomerization

The spectroscopically determined absorbance of a solution measures the *molar* concentration of the solute that absorbs the light of chosen wavelength. This is because, in the absence of anomalous effects due to changes in the molecular site of photon absorption, the Beer's Law diminution in the intensity of transmitted light depends on the number of solute molecules in the volume of solution defined by the transmission path of the light. Spectral studies invariably employ protein solutions sufficiently dilute for Beer's Law to be valid and, in the absence of other solutes, for thermodynamic ideality to be a reasonable assumption; in which case the choice of concentration scales (molar or molal) is academic. However, the need for consideration of nonideality effects arises when a high concentration of an inert cosolute is introduced as a molecular crowding agent [7] to displace the equilibrium towards the smaller isomeric state of the protein [3]. We therefore consider the effect of an inert cosolute  $M$  on the apparent isomerization constant under conditions wherein the protein concentration is sufficiently small in relation to that of  $M$  for the activity coefficients of the two isomeric states to be governed solely by the  $m_j$  term in Eq. (4). Under those conditions the equilibrium position of a protein isomerization reaction  $A \rightleftharpoons B$  is governed by

$$K_{molal}^{app} = m_B / m_A = K_{molal} \exp[(C_{AM} - C_{BM})m_M] \quad (7)$$

in which  $K_{molal} = a_B / a_A$ . After incorporation of Eq. (5a) and (5b), Eq. (7) becomes

$$\begin{aligned} K_{molal}^{app} &= K_{molal} \exp[(B_{AM} - M_A \bar{v}_A - B_{BM} + M_B \bar{v}_B)m_M \rho_s] \\ &= K_{molal} \exp[(B_{AM} - B_{BM})m_M \rho_s] \end{aligned} \quad (8)$$

where the simplified version takes into account the fact that the molar masses and partial specific volumes of the two isomeric states may both reasonably be identified with those of the protein. For the same reason it then follows from Eq. (6) that

$$K_{molal}^{app} = m_B / m_A = C_B / C_A = K_{molar}^{app} \quad (9)$$

In other words, the isomerization constant that is deduced from spectral studies on the basis of molar or the corresponding weight concentrations are numerically equal to the corresponding molal parameter. However, statistical-mechanical interpretation of the molecular crowding effect by the application of Eq. (8) clearly requires the inert solute concentration to be expressed on the molal ( $m_M \rho_s$ ) instead of the molar ( $C_M$ ) concentration scale.

## 2.2. Interaction involving two dissimilar macromolecular reactants

Because of the constraints of constant temperature and pressure that prevail in spectral studies, the interaction of a univalent ligand protein  $B$  with  $p$  sites on acceptor protein  $A$  is most appropriately described in terms of a binding function  $r$  (mol  $B$  bound per mol  $A$ ) on the molal concentration scale as

$$r = \frac{m_{AB} + 2m_{AB_2} + 3m_{AB_3} + \dots + pm_{AB_p}}{m_A + m_{AB} + m_{AB_2} + m_{AB_3} + \dots + m_{AB_p}} \quad (10)$$

For an ideal system with equivalence and independence of acceptor sites Eq. (10) becomes

$$r = \frac{pK_{molal}m_Am_B + 2[p(p-1)/2!]K_{molal}^2m_A^2m_B^2 + \dots + pK_{molal}^p m_A^p m_B^p}{m_A + [p(p-1)/2!]K_{molal}^2m_A^2m_B^2 + \dots + K_{molal}^p m_A^p m_B^p} \\ = \frac{pK_{molal}m_B}{1 + K_{molal}m_B} \quad (11)$$

where  $K_{molal}$  is the intrinsic binding constant [8]. Although spectral binding data are invariably interpreted in terms of molar ligand concentration  $C_B$  and the corresponding intrinsic binding constant ( $K_{molar}$ ), the essential identity of  $m_B\rho_S$  and  $C_B$  in dilute protein solution [Eq. (6)] renders  $K_{molal}$  an acceptable approximation of  $K_{molar}$  under conditions approaching thermodynamic ideality.

The inclusion of a high concentration  $m_M$  of inert solute  $M$  necessitates description of the various stepwise equilibria  $AB_{i-1} + B \rightleftharpoons AB_i$  in terms of thermodynamic activities in place of the molal concentrations employed in the expanded form of Eq. (11). In particular, the specification of equivalent and independent binding signifies conformity with the following series of relationships between the intrinsic binding constant and species involved in the successive equilibrium steps.

$$K_{molal} = \frac{a_{AB}}{a_A(a_B)^i} = \frac{m_{AB}\Gamma_i}{m_A(m_B)^i}; \quad 1 \leq i \leq p \quad (12a)$$

$$\Gamma_i = y_{AB_i} / [y_A(y_B)^i] \quad (12b)$$

where simplification to the rectangular hyperbolic counterpart of Eq. (11), namely

$$r = \frac{pK_{molal}m_B\Gamma}{1 + K_{molal}m_B\Gamma} \quad (13)$$

is conditional upon conformity of the various activity coefficient ratios with the relationship

$$\Gamma_i = \Gamma^i \quad (14)$$

where  $\Gamma \equiv \Gamma_1$  is defined by Eq. (12b) with  $i = 1$ . Before its adoption, the validity of this assumption clearly needs to be examined closely for the particular system under investigation (see later).

### 3. Applications

We commence this section by considering the effects of high concentrations of inert cosolutes on the reversible unfolding of proteins, where displacement of the isomeric equilibrium is monitored readily by difference spectroscopy [4,5,9–13]. Results for the temperature-induced unfolding of  $\alpha$ -chymotrypsin [4] are used as the illustrative example.

#### 3.1. Effect of sucrose concentration on the reversible unfolding of $\alpha$ -chymotrypsin

Under acidic conditions (pH 2–3)  $\alpha$ -chymotrypsin undergoes a conformational change that is readily detected by difference spectroscopy [9,10]. The suppression of this temperature-induced reversible unfolding by high concentrations of sucrose [4] was attributed to preferential solvation of the more compact, folded state of the enzyme; but those findings are also amenable to statistical-mechanical interpretation as a consequence of thermodynamic nonideality [5]. Both interpretations rely upon Van't Hoff plots for the thermal denaturation of  $\alpha$ -chymotrypsin having the same slopes in the absence and presence of sucrose (Fig. 4a of [4]) – an observation which signifies the absence of an enthalpic contribution to the change

in isomerization constant, and hence justifies consideration of its dependence upon sucrose concentration to be entropy driven.

The effect of sucrose on the isomerization constant at 50 °C is summarized in Fig. 1, where the results (●) are plotted in accordance with the logarithmic form of Eq. (8). Also shown is the corresponding dependence (○) with concentrations of sucrose erroneously expressed on a molar rather than a molal basis. Whereas the slope of that dependence was taken [5] to signify a magnitude of  $-4.2$  L/mol for  $(B_{AM} - B_{BM})$ , the correct value is now seen to be  $-3.4$  L/mol (the slope of the solid line in Fig. 1). The difference between the sizes of the compact (native) and unfolded isomeric states of  $\alpha$ -chymotrypsin is thus smaller than previously envisaged [5].

The absence of net charge on sucrose ( $M$ ) allows identification of the second virial coefficient for excluded-volume interaction between solute and enzyme states ( $B_{iM}$ ) with the covolume [14],

$$B_{iM} = 4\pi L(R_i + R_M)^3 / 3; \quad i = A \text{ or } B \quad (15)$$

where  $R_j$  denotes a species radius; and where Avogadro's number ( $L$ ) has been included to convert covolumes from a molecular to a molar basis. Substituting effective radii of 2.44 and 0.31 nm for native chymotrypsin [15] and sucrose [3] respectively gives rise to an estimate of 52.4 L/mol for  $B_{AM}$ , whereupon  $B_{BM} = 55.8$  L/mol. On the basis of the value of 2.81 nm that is then calculated for  $(R_B + R_M)$ , the unfolded state is characterized by an effective radius that is 2.4% larger than that of native enzyme (2.50 cf 2.44 nm). Similar calculations with the slightly larger value of 56.6 L/mol for  $B_{BM}$  that is inferred from the incorrect estimate of  $(B_{AM} - B_{BM})$  signify an effective radius of 2.51 nm for the unfolded enzyme state. Whether the isomeric transition being characterized by difference spectroscopy should be regarded as reflecting a 7.7% or 9.0% expansion of the enzyme is clearly not a critical issue. However, the former represents the more rigorous statistical-mechanical interpretation of the effect of sucrose on the reversible unfolding of  $\alpha$ -chymotrypsin.

#### 3.2. Effect of inert polymers on the binding of superoxide dismutase to catalase

A recent publication [6] has employed fluorescence quenching to characterize the effect of polymeric cosolutes (Dextran 70 and PEG 2000) on the binding of superoxide dismutase to catalase. Those results are now re-examined to illustrate application of the theoretical expressions presented in Section 2.2.

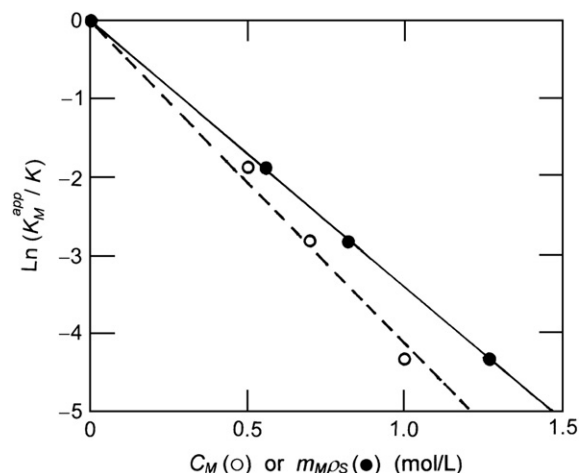


**Fig. 1.** Effect of concentration scale used to estimate the molar covolume difference,  $(B_{AM} - B_{BM})$ , from the effect of sucrose concentration on the isomerization constant for the reversible unfolding of  $\alpha$ -chymotrypsin. ○, Earlier interpretation [5] of results taken from Fig. 4a of [4]; ●, current interpretation with molality recognized as the appropriate concentration scale for defining thermodynamic activity in spectral studies.

The first point to note is that in spectral studies the binding function (or fractional site saturation) should be defined on the molal scale because of the constant pressure constraint that applies to measurements of fluorescence quenching [Eq. (11)]. Although the intrinsic binding constant defined on a molar basis can be taken as the corresponding molal parameter in the absence of cosolute, that measured in the presence of a high cosolute concentration needs correction to the molal scale. Inasmuch as

$$K_{\text{molal}}^{\text{app}} = K_{\text{molar}}^{\text{app}}(1 - M_M \bar{v}_M C_M) \rho_S \quad (16)$$

the molar intrinsic association constant determined in the presence of a concentration  $C_M$  of cosolute overestimates slightly the magnitude of  $K_{\text{molal}}^{\text{app}}$ , whereupon the experimental values of  $\ln \Gamma = \ln(K_{\text{molal}}^{\text{app}}/K_{\text{molar}})$  reported in Fig. 2 of [6] require modification to incorporate the  $\ln[(1 - M_M \bar{v}_M C_M) \rho_S]$  correction factor. Those corrections have been based on respective partial specific volumes of 0.611 and 0.84 mL/g for Dextran 70 [16] and PEG 2000 [17], together with an assumed buffer density ( $\rho_S$ ) of 1 kg/L.

Secondly, statistical-mechanical prediction of nonideality arising from the presence of a high concentration of cosolute (presumed inert) requires account to be taken of the consequences of Eq. (5a), which signifies the need to include molar volume terms ( $M_M \bar{v}_M C_M$ ) in the ratio of molal activity coefficients  $y_{AB}/y_{AV}y_B$  expressed in terms of the osmotic second virial coefficients ( $B_{AB}$ , etc.) that arise in statistical-mechanical interpretation of thermodynamic nonideality. An additional factor to be considered is the reliability of the approximation inherent in Eq. (14) that each successive equilibrium step is described by a common activity coefficient ratio  $\Gamma$  for the binding of superoxide dismutase to multiple sites on catalase. Inasmuch as catalase is a tetramer of 60 kDa subunits it is necessary to accommodate the possible attachment of four molecules

of superoxide dismutase ( $M_B = 33$  kDa) in a series of successive equilibria.

Because the expressions for the activity coefficients of the interacting species are all dominated by the  $C_{iM}m_M$  term it follows that

$$\Gamma_i = \exp[(C_{AM} + iC_{BM} - C_{AB,M})m_M + \dots] \quad (17)$$

or, in terms of osmotic second virial coefficients [Eq. (5a)],

$$\Gamma_i = \exp[(B_{AM} + iB_{BM} - B_{AB,M} - iM_M \bar{v}_M)m_M \rho_S + \dots] \quad (18)$$

As noted in Section 2.2, simplification of the binding equation to a rectangular hyperbolic dependence upon  $m_B \rho_S$  entails the assumption that the activity coefficient ratio  $\Gamma_i$  conform with Eq. (14), whereupon its logarithmic counterpart,

$$\ln \Gamma_i = i \ln \Gamma \quad (19)$$

predicts a linear dependence of  $\ln \Gamma_i$  upon stoichiometry of the complex. The slope of that dependence ( $S$ ) then identifies the coefficient of the exponent in the expression

$$\Gamma = \exp(Sm_M \rho_S + \dots) \quad (20)$$

for the activity coefficient ratio relating the apparent and thermodynamic intrinsic association constants ( $K_{\text{molal}}^{\text{app}}/K_{\text{molal}}$ ).

The likely validity of that assumption is now examined by calculating second virial coefficients for all reactant and product species on the basis that the absence of charge on either cosolute allows the identification of  $B_{iM}$  with the corresponding covolume [Eq. (15)]. An effective radius ( $R_M$ ) of 7.0 nm has been calculated for Dextran 70 from the relationship  $R_M = 0.0271M_M^{0.48}$  [18], the corresponding value for PEG 2000 being 1.3 nm on the basis of the relationship  $R_M = 0.0292\sqrt{M_M}$  [19]. Parameters used and the results obtained from those calculations are summarized in Table 1, about which the following points require comment. The effective radii reported for the two reactants are Stokes radii deduced from sedimentation velocity studies of catalase [20] and superoxide dismutase [21,22], whereas those for the four putative complexes are based on assumed spherical geometry and conservation of molar volume  $V$ : thus  $R_{AB_i} = [3(V_A + iV_B)/(4\pi L)]^{1/3}$ . Values of the resulting second virial coefficients [Eq. (15)] are listed in the right-hand columns of Table 1.

The validity of assuming conformity of the activity coefficient ratios with Eq. (19) is supported by the essentially linear plots shown in Fig. 2A and B, the slopes of which signify that the coefficients of the exponent ( $S$ ) in Eq. (20) are 2074 ( $\pm 7$ ) and 89 ( $\pm 1$ ) L/mol for Dextran 70 and PEG 2000 respectively. In view of this substantiation

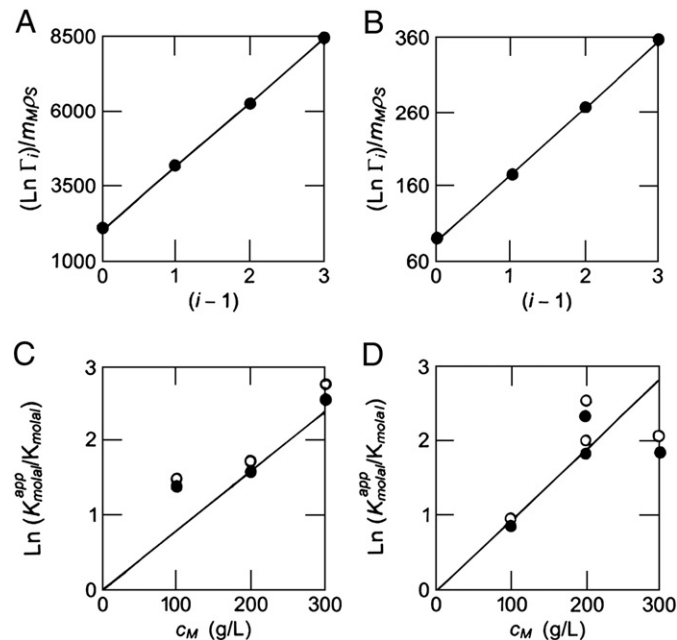


**Fig. 2.** Reinterpretation of results from a fluorescence quenching study [6] of the effects of polymeric cosolutes on the interaction between catalase and superoxide dismutase. A and B: Tests of the likely validity of assuming that the activity coefficient ratios ( $\Gamma_i$ ) for successive steps of the reaction are describable in terms of Eqs. (18) and (19) in studies with Dextran 70 and PEG 2000 as the respective cosolutes (values of the various virial coefficients given in Table 1). C and D: Consequent reassessments of the respective results for the catalase–dismutase interaction: ○, data reported in Fig. 2 of [6] based on the assumption that molarity is the appropriate concentration scale; ●, revised estimates of  $\ln \Gamma$  based on Eq. (16). Solid lines depict the theoretical dependencies predicted by Eq. (20) with  $S$  taken as the slopes from Fig. 2A and B for studies with Dextran 70 and PEG 2000 as the respective cosolute (see text).

**Table 1**

Parameters used for the calculation of osmotic second virial coefficients ( $B_{iM}$ ) for interactions of the various species ( $i$ ) in the catalase–superoxide dismutase system with inert cosolute  $M$ .

| Species $i$     | Effective radius $R_i^a$ (nm) | Second virial coefficient $B_{iM}$ (L/mol) <sup>b</sup> |          |
|-----------------|-------------------------------|---|----------|
|                 |                               | Dextran 70  | PEG 2000 |
| Catalase (A)    | 5.30 [17]                     | 4690  | 725      |
| Dismutase (B)   | 2.80 [18, 19]                 | 2370  | 174      |
| AB              | 5.55                          | 4980  | 811      |
| AB <sub>2</sub> | 5.78                          | 5260  | 895      |
| AB <sub>3</sub> | 5.99                          | 5530  | 977      |
| AB <sub>4</sub> | 6.18                          | 5990  | 1055     |

<sup>a</sup> Values for the two reactants taken as the Stokes radii deduced from the indicated sources, those for the four putative complexes being based on spherical geometry and conservation of volume.

<sup>b</sup> Calculated from Eq. [15] on the basis of effective radii of 7.0 and 1.3 nm for Dextran 70 and PEG 2000 respectively.



of the interpretation the fluorescence quenching data [6] in terms of Eq. (13), the evaluation of an intrinsic association constant from fractional saturation data ( $r/p$ ) becomes independent of the actual number of catalase sites to which superoxide dismutase binds. Comparison of the predicted dependencies of  $\ln(K_{\text{molal}}^{\text{app}}/K_{\text{molal}})$  upon the concentrations of Dextran 70 and PEG 2000 (solid lines) with the experimental results is shown in Fig. 2C and D respectively, where open symbols denote the reported values (Fig. 2 of [6]) and solid symbols their corrected counterparts [Eq. (16)]. Although the correction is relatively small, the revised values provide the more rigorous estimates of  $\ln\Gamma$ , which conform reasonably well with description of the thermodynamic nonideality on the statistical-mechanical basis of excluded volume.

The above conformity should not be construed as unequivocal evidence that the effect of cosolute addition is purely entropic. Indeed, results obtained at a series of temperatures have signified the superimposition of an enthalpic contribution to the energetics [6] – a finding that questions the inertness of the two space-filling cosolutes. In that regard the necessity to invoke chemical reactivity of the molecular-crowding cosolute has also been proposed as the source of the disparity between predicted and experimentally observed dependences of the enhancement of complex formation between dissimilar species ( $A + B \rightleftharpoons C$ ) upon the molecular mass of polyethylene glycol used to displace the equilibrium [23,24]. Indeed, the findings for the catalase–superoxide dismutase system [6] again draw attention to the fact that excluded volume is not the sole determinant of the consequences of protein–polymer interaction because of the potential for involvement of the polyethylene glycol repeat unit ( $-\text{CH}_2\text{CH}_2-\text{O}-$ ) in hydrogen bonding as well as hydrophobic interaction [17,25–27].

#### 4. Concluding remarks

This investigation has drawn attention to the fact that thermodynamic activity is properly defined on the molal concentration scale in experiments conducted under the constraints of constant temperature and pressure. Also illustrated is a means of restoring thermodynamic rigor to the characterization of protein interactions from results mistakenly represented using the molar scale as the independent variable. Although that reanalysis has led to only minor refinement of the quantitative interpretation for the two systems used to illustrate the correction process, it is clearly preferable to avoid the necessity for such molar–molal interconversions by adopting the more appropriate concentration scale at the outset in experimental studies requiring consideration of thermodynamic nonideality when constancy of temperature and pressure are the operative constraints in the monitoring of solute chemical potentials.

#### Acknowledgments

PRW thanks The University of Auckland for the use of office, library and computing facilities.

#### References

- [1] T.L. Hill, Theory of solutions. I, *J. Am. Chem. Soc.* 79 (1957) 4885–4890.
- [2] T.L. Hill, *Thermodynamics for Chemists and Biologists*, Addison–Wesley, Reading, MA, 1968.
- [3] D.J. Winzor, P.R. Wills, Thermodynamic nonideality and protein solvation, in: R.B. Gregory (Ed.), *Protein–Solvent Interactions*, Marcel Dekker, New York, 1995, pp. 483–520.
- [4] J.C. Lee, S.N. Timasheff, The stabilization of proteins by sucrose, *J. Biol. Chem.* 256 (1981) 7193–7201.
- [5] D.J. Winzor, P.R. Wills, Effects of thermodynamic nonideality on protein interactions: equivalence of interpretations based on excluded volume and protein solvation, *Biophys. Chem.* 25 (1986) 243–251.
- [6] M. Jiao, H.-T. Li, J. Chen, A.P. Minton, Y. Liang, Attractive protein–polymer interactions markedly alter the effect of macromolecular crowding on protein association equilibria, *Biophys. J.* 99 (2010) 914–923.
- [7] A.P. Minton, The effect of volume occupancy upon the thermodynamic activity of proteins: some biochemical consequences, *Mol. Cell. Biochem.* 55 (1983) 119–140.
- [8] I.M. Klotz, The application of the law of mass action to binding by proteins: interactions with calcium, *Arch. Biochem.* 9 (1946) 109–117.
- [9] B.H. Havsteen, G.P. Hess, Evidence for conformational changes in  $\alpha$ -chymotrypsin-catalyzed reactions. VII. Thermal induced reversible changes in conformation at pH 2.0, *J. Am. Chem. Soc.* 85 (1963) 796–802.
- [10] R. Biltonen, R. Lumry, Studies of the chymotrypsinogen family of proteins. VI. Characterization of the conformational variation of chymotrypsin, *J. Am. Chem. Soc.* 91 (1969) 4251–4256.
- [11] K.E. Shearwin, D.J. Winzor, Thermodynamic nonideality as a probe of reversible protein unfolding effected by variations in pH and temperature: studies of ribonuclease, *Arch. Biochem. Biophys.* 282 (1990) 297–301.
- [12] P.R. Davies-Searle, A.S. Morar, A.J. Saunders, D.A. Erie, G.J. Pielak, Sugar-induced molten–globule model, *Biochemistry* 37 (1998) 17048–17053.
- [13] A.J. Saunders, P.R. Davies-Searle, D.L. Allen, G.J. Pielak, D.A. Erie, Osmolyte-induced changes in protein conformational equilibria, *Biopolymers* 53 (2000) 293–307.
- [14] W.G. McMillan, J.E. Mayer, The statistical thermodynamics of multicomponent systems, *J. Chem. Phys.* 13 (1945) 276–305.
- [15] M.P. Jacobsen, D.J. Winzor, Refinement of the omega analysis for the quantitative characterization of solute self-association by sedimentation equilibrium, *Biophys. Chem.* 45 (1992) 119–132.
- [16] K.A. Granath, Solution properties of branched dextrans, *J. Colloid Sci.* 13 (1958) 308–328.
- [17] L.S. Sandell, D.A.J. Goring, Correlation between the temperature dependence of apparent specific volume and the conformation of oligomeric propylene glycols in aqueous solution, *J. Polym. Sci., A-2 Polym. Phys.* 9 (1971) 115–126.
- [18] P. DePhillips, A.M. Lenhoff, Pore size distributions of cation-exchange adsorbents determined by size-exclusion chromatography, *J. Chromatogr. A* 883 (2000) 39–54.
- [19] D.H. Atha, K.C. Ingham, Mechanism of precipitation of proteins by polyethylene glycols in terms of excluded volume, *J. Biol. Chem.* 256 (1981) 12108–12117.
- [20] H. Sund, K. Weber, E. Mölbert, Dissoziation der rinderleber katalase in ihre untereinheiten, *Eur. J. Biochem.* 1 (1967) 400–410.
- [21] J.W. Hartz, H.F. Deutsch, Preparation and physicochemical properties of human erythrocyte, *J. Biol. Chem.* 244 (1969) 4565–4572.
- [22] J.M. McCord, I. Fridovich, Superoxide dismutase: an enzyme function for erythrocyte (hemocuprein), *J. Biol. Chem.* 244 (1969) 6049–6055.
- [23] D.J. Winzor, P.R. Wills, Molecular crowding effects of linear polymers in protein solutions, *Biophys. Chem.* 119 (2006) 186–195.
- [24] M.K. Reddy, S.E. Weitzel, S.S. Daube, T.C. Jarvis, P.H. von Hippel, Using macromolecular crowding agents to identify weak interactions within DNA replication complexes, *Methods Enzymol.* 262 (1995) 466–476.
- [25] B.E. Michel, M.R. Kaufman, The osmotic potential of polyethylene glycol 6000, *Plant Physiol.* 51 (1973) 914–916.
- [26] D.J. Winzor, Reappraisal of disparities between osmolality estimates by freezing point depression and vapor pressure deficit methods, *Biophys. Chem.* 107 (2004) 317–323.
- [27] G. Tubio, B. Nerli, G. Picó, Relationship between the protein surface hydrophobicity and its partition behavior in aqueous two-phase systems of polyethylene glycol–dextran, *J. Chromatogr. B Biomed. Sci. Appl.* 799 (2004) 293–301.